

**Duality and the universality class of the three-state Potts antiferromagnet on plane quadrangulations**Jian-Ping Lv,<sup>1,2,\*</sup> Youjin Deng,<sup>3,4,†</sup> Jesper Lykke Jacobsen,<sup>5,6,7,‡</sup> Jesús Salas,<sup>8,9,§</sup> and Alan D. Sokal<sup>10,11,||</sup><sup>1</sup>*Department of Physics, Anhui Normal University, Wuhu 241000, China*<sup>2</sup>*Anhui Province Key Laboratory of Optoelectric Materials Science and Technology, Wuhu 241000, China*<sup>3</sup>*Hefei National Laboratory for Physical Sciences at Microscale and Department of Modern Physics, University of Science and Technology of China, Hefei, Anhui 230026, China*<sup>4</sup>*CAS Center for Excellence and Synergetic Innovation Center in Quantum Information and Quantum Physics, University of Science and Technology of China, Hefei, Anhui 230026, China*<sup>5</sup>*Laboratoire de Physique Théorique, Département de Physique de l'ENS, École Normale Supérieure, Sorbonne Université, CNRS, PSL Research University, 75005 Paris, France*<sup>6</sup>*Sorbonne Université, École Normale Supérieure, CNRS,**Laboratoire de Physique Théorique (LPT ENS), 75005 Paris, France*<sup>7</sup>*Institut de Physique Théorique, CEA Saclay, 91191 Gif-sur-Yvette, France*<sup>8</sup>*Grupo de Modelización, Simulación Numérica y Matemática Industrial, Universidad Carlos III de Madrid, Avenida de la Universidad 30, 28911 Leganés, Spain*<sup>9</sup>*Grupo de Teorías de Campos y Física Estadística, Instituto Gregorio Millán, UC3M, Unidad Asociada al IEM-CSIC, Madrid, Spain*<sup>10</sup>*Department of Physics, New York University, 4 Washington Place, New York, NY 10003, USA*<sup>11</sup>*Department of Mathematics, University College London, Gower Street, London WC1E 6BT, United Kingdom*

(Received 19 December 2017; revised manuscript received 6 February 2018; published 25 April 2018)

We provide a criterion based on graph duality to predict whether the three-state Potts antiferromagnet on a plane quadrangulation has a zero- or finite-temperature critical point, and its universality class. The former case occurs for quadrangulations of self-dual type, and the zero-temperature critical point has central charge  $c = 1$ . The latter case occurs for quadrangulations of non-self-dual type, and the critical point belongs to the universality class of the three-state Potts ferromagnet. We have tested this criterion against high-precision computations on four lattices of each type, with very good agreement. We have also found that the Wang-Swendsen-Kotecký algorithm has no critical slowing-down in the former case, and critical slowing-down in the latter.

DOI: [10.1103/PhysRevE.97.040104](https://doi.org/10.1103/PhysRevE.97.040104)**I. INTRODUCTION**

Ever since Kramers and Wannier's [1] pioneering work on the two-dimensional (2D) Ising model, the concept of duality has led to important insights in statistical mechanics and quantum field theory [2] and more recently also in string theory [3]. The purpose of this Rapid Communication is to show an unusual application of duality to the study of the three-state Potts antiferromagnet (AF) on a class of 2D lattices.

The  $q$ -state Potts model [4,5] plays a key role in the theory of critical phenomena, especially in 2D [6–8], and has applications to various condensed-matter systems [5]. Ferromagnetic Potts models are by now fairly well understood, owing to universality; but the behavior of AF Potts models depends strongly on the microscopic lattice structure, so that many basic questions about the phase diagram and critical exponents must be investigated case by case. One expects that for each lattice  $\mathcal{L}$  there exists a value  $q_c(\mathcal{L})$  (possibly noninteger) such that for

$q > q_c(\mathcal{L})$  the model has an exponential decay of correlations at all temperatures  $T$  including zero, while for  $q = q_c(\mathcal{L})$  the model has a zero-temperature critical point. The first task, for any lattice, is thus to determine  $q_c$ .

Some 2D AF models at  $T = 0$  have the remarkable property that they can be mapped exactly onto a “height” model (in general, vector valued) [9–13]. Since the height model must either be in a “smooth” (ordered) or “rough” (massless) phase, the corresponding zero-temperature spin model must either be ordered or critical, never disordered. When the height model is critical, the long-distance behavior is that of a massless Gaussian with some (*a priori* unknown) “stiffness matrix”  $\mathbf{K} > \mathbf{0}$ . The critical operators can be identified via the height mapping, and the corresponding critical exponents can be predicted in terms of  $\mathbf{K}$ . Height representations thus provide a means for recovering a sort of universality for some (but not all) AF models and for understanding their critical behavior in terms of conformal field theory (CFT).

In particular, on any plane quadrangulation (i.e., any planar lattice in which all faces are quadrilaterals), the three-state Potts AF at  $T = 0$  admits a height mapping [12,14]. But is this model critical, or is it ordered? For the square lattice it is known [11,12,15,16] that the zero-temperature model is critical, so that  $q_c = 3$ . By contrast, for the diced lattice it can be rigorously proven [14,17] that there is a finite-temperature

\*phys.lv@gmail.com

†yjdeng@ustc.edu.cn

‡jesper.jacobsen@ens.fr

§jsalas@math.uc3m.es

||sokal@nyu.edu

phase transition, with an ordered phase at all low temperatures, so that  $q_c > 3$  (numerical estimates from transfer matrices yield  $q_c(\text{diced}) \approx 3.45$  [18]). Moreover, we have recently [19] given examples of plane quadrangulations in which  $q_c$  takes arbitrarily large values. It is thus of interest to find conditions on the quadrangulation telling us whether the three-state Potts AF at  $T = 0$  is critical or ordered.

In this Rapid Communication we shall propose a criterion, involving graph duality, that appears to give a precise solution to this problem.

Recall first that, for any (finite or infinite) graph  $G = (V, E)$  embedded in the plane, the dual graph  $G^* = (V^*, E^*)$  is defined by placing a vertex in each face of  $G$  and drawing an edge  $e^*$  across each edge  $e$  of  $G$ . Since  $G^{**} = G$ , we refer to the pair  $(G, G^*)$  as a *dual pair*. A graph  $G$  is called *self-dual* if  $G$  is isomorphic to  $G^*$ .

Now consider a plane quadrangulation  $\Gamma = (V, E)$ . Since it is bipartite (say,  $V = V_0 \cup V_1$ ), we may define sublattices  $G_0 = (V_0, E_0)$  and  $G_1 = (V_1, E_1)$  by drawing edges across the diagonals of the quadrilateral faces; it is easy to see that  $G_0$  and  $G_1$  form a dual pair. Conversely, given a dual pair  $(G_0, G_1)$  of plane graphs, we can construct a quadrangulation  $\mathcal{Q}(G_0) = \mathcal{Q}(G_1)$  with the vertex set  $V = V_0 \cup V_1$  by connecting each vertex in  $G_0$  to the neighboring vertices in  $G_1$ . There is thus a one-to-one correspondence between quadrangulations  $\Gamma$  and dual pairs of plane graphs  $(G_0, G_1)$ . We shall say that the quadrangulation  $\mathcal{Q}(G_0)$  is of *self-dual type* if  $G_0$  is self-dual, and of *non-self-dual type* otherwise. For instance, the square lattice is a quadrangulation of self-dual type (both  $G_0$  and  $G_1$  are themselves square lattices), while the diced lattice is a quadrangulation of non-self-dual type (the sublattices are triangular and hexagonal).

Let us henceforth restrict attention to periodic planar lattices. It is well known (and obvious) that the square lattice is self-dual; what seems to be less well known is that there exist infinitely many examples of self-dual periodic planar lattices [20–26], including the “hextri” lattice see Figs. 1 and 10 in Ref. [21], Fig. 16 in Ref. [23], and Fig. 1(b) in Ref. [24], the “house” lattice (see Fig. 2 in Ref. [21]), the martini-B lattice (see Fig. 8 in Ref. [25]), and the cmm-pmm lattice (see Fig. 29 in Ref. [23]). In particular, from each of these lattices we can construct the corresponding quadrangulation of self-dual type.

In this Rapid Communication we present the results of our study—using Monte Carlo (MC), transfer matrices (TMs), and critical polynomials (CPs) [27]—of the three-state Potts AF on a variety of quadrangulations of both types. We find empirically, without exception, the following behavior:

*Conjecture 1.* For the three-state Potts AF on a (periodic) plane quadrangulation  $\Gamma$ :

(1) If  $\Gamma$  is of self-dual type, the model has a zero-temperature critical point, so that  $q_c = 3$ . This critical point has central charge  $c = 1$ .

(2) If  $\Gamma$  is of non-self-dual type, the model has a finite-temperature phase transition, so that  $q_c > 3$ . This transition is second order and lies in the universality class of the three-state Potts ferromagnet.

Four AF Potts models on planar lattices with a critical point at  $T = 0$  are known [9,12]: the square and kagome lattices with  $q = 3$ , and the triangular lattice with  $q = 2$  and  $q = 4$ . By contrast, Conjecture 1 implies that this phenomenon is

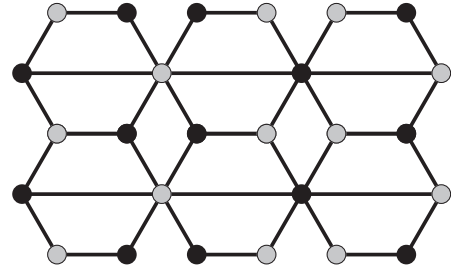


FIG. 1. The quadrangulation  $\mathcal{Q}(\text{hextri})$ .

not so exceptional: There are infinitely many  $q = 3$  models displaying it.

We have studied four quadrangulations of self-dual type:  $\mathcal{Q}(\text{hextri})$  (see Fig. 1),  $\mathcal{Q}(\text{house})$ ,  $\mathcal{Q}(\text{martini-B})$ , and  $\mathcal{Q}(\text{cmm-pmm})$ . We have also considered four quadrangulations of non-self-dual type:  $\mathcal{Q}(\text{diced})$  (see Fig. 2),  $\mathcal{Q}(\text{martini})$ ,  $\mathcal{Q}(\text{ruby})$ , and  $G'_3$  [see Fig. 2(b) in Ref. [19]]. As the qualitative behavior of the four lattices within each class turns out to be the same, we refrain from giving here all the details [28], and shall focus on one lattice of each type:  $\mathcal{Q}(\text{hextri})$  and  $\mathcal{Q}(\text{diced})$ .

## II. QUADRANGULATIONS OF SELF-DUAL TYPE

If the quadrangulation is of self-dual type, then we expect the number of ideal states [9,12] to be six: The system must choose which of the two sublattices to order, and in which of the three possible spin directions. It is therefore natural to expect (by using universality arguments) that, as for the square lattice, there will be a critical point at  $T = 0$  characterized by a CFT with central charge  $c = 1$  [28].

We first investigated the three-state Potts AF by extensive MC simulations on lattices of size  $L \times L$  unit cells with periodic boundary conditions (BCs), using the Wang-Swendsen-Kotecký (WSK) cluster algorithm [29]. As our lattices are bipartite, this algorithm is known to be ergodic even at  $T = 0$  [11,30,31]. For each lattice, we measured the staggered and uniform susceptibilities, which are expected to diverge at the critical point as  $\chi_{\text{stagg}} \sim L^{(\gamma/\nu)_{\text{stagg}}}$  and  $\chi_{\text{u}} \sim L^{(\gamma/\nu)_{\text{u}}}$ . The qualitative behavior of these susceptibilities is the same for all four lattices considered here, but the critical exponents  $(\gamma/\nu)_{\text{stagg}}$  and  $(\gamma/\nu)_{\text{u}}$  do depend on the lattice. In Fig. 3 we show, as an example, the scaled staggered susceptibility on the  $\mathcal{Q}(\text{hextri})$  lattice (we use, instead of the standard Potts-model coupling constant  $J$ , the variable  $v = e^J - 1$ ). All the finite- $L$  curves meet at  $v = -1$ , implying that this point is indeed critical.

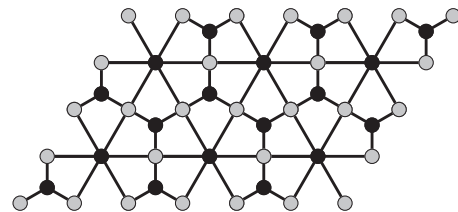


FIG. 2. The quadrangulation  $\mathcal{Q}(\text{diced})$ , which is also the Laves lattice  $D(3,4,6,4)$  and is the dual of the ruby lattice. The black (gray) vertices form a diced (kagome) sublattice.

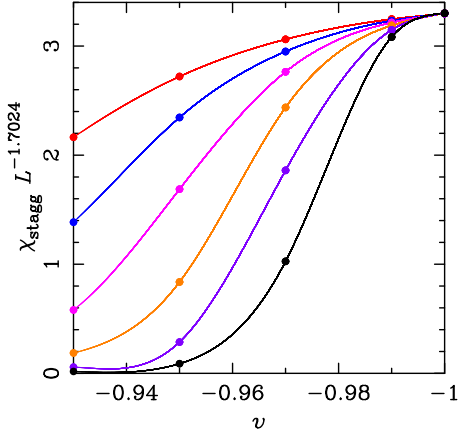


FIG. 3. The scaled staggered susceptibility for the  $\mathcal{Q}(\text{hextri})$  lattice as a function of  $v = e^J - 1$  in the region close to  $v = -1$ . We show the data (from top to bottom) for  $L = 32$  (red),  $L = 64$  (blue),  $L = 128$  (pink),  $L = 256$  (orange),  $L = 512$  (violet), and  $L = 1024$  (black). The curves are spline-interpolation curves to guide the eye.

The height representation [9–12] relates these susceptibility exponents to the stiffness  $K$  (which is a scalar in this case),

$$(\gamma/v)_{\text{stagg}} = 2 - \frac{\pi}{18K}, \quad (\gamma/v)_u = 2 - \frac{2\pi}{9K}. \quad (1)$$

The results for the four lattices studied here, along with the known exact values for the square lattice [11, 12], are displayed in Table I. The value of the stiffness is in all cases much smaller than the critical value  $K_c = \pi/2 \approx 1.570796$  where the locking potential becomes marginal, which separates the rough and smooth phases [9, 10, 12].

We also found that, for all these lattices, the WSK algorithm does not suffer from critical slowing-down (CSD). By measuring the integrated autocorrelation times  $\tau_{\text{int}}$  for the staggered and uniform susceptibilities at  $T = 0$ , we find that  $\tau_{\text{int}} \lesssim 8$  uniformly in  $L$ . This phenomenon also occurs for the square-lattice model [12, 30]. We conjecture that the WSK algorithm for the three-state Potts AF on any quadrangulation of self-dual type has no CSD.

We also studied the  $\mathcal{Q}(\text{hextri})$  lattice by means of a TM approach. We considered strip graphs of this lattice with cylindrical BC and widths  $2 \leq L \leq 14$ . In Fig. 1, our TM propagates from left to right. We measured the free energy (per unit area)  $f_L(q)$  at  $T = 0$  in the AF regime for  $2 \leq q \leq 4$ . The

TABLE I. Critical exponents  $(\gamma/v)_{\text{stagg}}$  and  $(\gamma/v)_u$ , and the estimated stiffness  $K$ , for the zero-temperature three-state Potts AF on the quadrangulations  $\Gamma$  of self-dual type studied in this Rapid Communication. We include for comparison the exact values for the square lattice [12].

$\Gamma$	$(\gamma/v)_{\text{stagg}}$	$(\gamma/v)_u$	$K$
$\mathcal{Q}(\text{cmm-pmm})$	1.71762(9)	0.8691(5)	0.6177(6)
$\mathcal{Q}(\text{hextri})$	1.7024(3)	0.8096(9)	0.5865(6)
$\mathcal{Q}(\text{house})$	1.6978(3)	0.7922(4)	0.5778(8)
$\mathcal{Q}(\text{martini-B})$	1.6882(3)	0.7557(9)	0.5609(6)
Square	5/3	2/3	$\pi/6$

TABLE II.  $q_{\text{max}}(L)$  and  $c_{\text{max}}(L)$  for the  $T = 0$   $q$ -state Potts AF on the  $\mathcal{Q}(\text{hextri})$  lattice with cylindrical BC as a function of the width  $L$ , and the extrapolation to  $L = \infty$ .

$L$	$q_{\text{max}}(L)$	$c_{\text{max}}(L)$
2	3.8544146155	0.8508786050
4	3.2788982545	1.0133854086
6	3.1443621430	1.0588380075
8	3.0975518402	1.0554325766
10	3.0795627986	1.0383006482
$\infty$	3.00(2)	0.99(2)

central charge  $c(q)$  can be extracted using the standard CFT ansatz [32, 33]

$$f_L(q) = f_{\text{bulk}}(q) - \frac{c(q)\pi}{6L^2} + o(L^{-2}). \quad (2)$$

We first observed that there are parity effects depending on the value of  $L \bmod 4 = 0, 2$ . We then ignored the  $o(L^{-2})$  terms, fitted the values corresponding to  $L, L + 4$  to (2), and extracted the estimates  $c_L(q)$ . This curve exhibits, for each value of  $L$ , a maximum value  $c_{\text{max}}(L)$  at  $q = q_{\text{max}}(L)$ . These values are displayed in Table II, together with our extrapolations to  $L = \infty$  (see details of the fits in Ref. [28]). These results agree well with our conjecture that the  $q = 3$  Potts AF on  $\mathcal{Q}(\text{hextri})$  is critical at  $T = 0$ , with behavior described by a CFT with  $c = 1$ .

### III. QUADRANGULATIONS OF NON-SELF-DUAL TYPE

When the quadrangulation is of non-self-dual type, the asymmetry between the two sublattices suggests that at  $T = 0$  one preferred sublattice will be ordered (in one of the three possible spin directions) and the other sublattice disordered (between the other two states). If this is so, then at  $T = 0$  there are only three ideal states, each of them with one sublattice ferromagnetically ordered. Therefore, we have the same  $\mathbb{Z}_3$  symmetry and ground-state degeneracy as for the three-state Potts ferromagnet, and hence we expect a finite-temperature second-order transition in the universality class of this latter model. However, a first-order finite-temperature transition is also possible.

In particular, if the two sublattices have unequal vertex densities (as occurs most often), then we expect that the sublattice with the smaller (larger) vertex density will be ordered (disordered), as this maximizes the entropy. The reasoning becomes more subtle, however, if the two sublattices have equal vertex densities [as occurs, for instance, for  $\mathcal{Q}(\text{diced})$  and  $\mathcal{Q}(\text{ruby})$ ]: Then it is not obvious how the asymmetry alone can drive the phase transition. For this reason we focus here on  $\mathcal{Q}(\text{diced})$ .

Once again we studied the three-state Potts AF using MC simulations on lattices of size  $L \times L$  unit cells with periodic BC, using the WSK algorithm. In all cases, we find a finite-temperature critical point. We followed the practical methods of Ref. [14] to locate the critical point, and then fitted our numerical data to the finite-size-scaling (FSS) ansatz

$$\mathcal{O}_L = L^{p_0} [\mathcal{O}_c + a_1(v - v_c)L^{1/\nu} + a_2(v - v_c)^2 L^{2/\nu} + b_1 L^{-\omega_1} + \dots]. \quad (3)$$

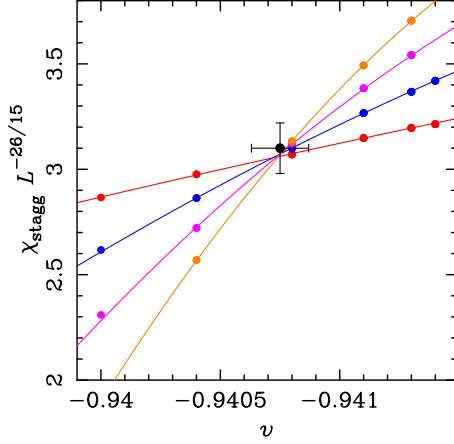


FIG. 4. The scaled staggered susceptibility for the  $\mathcal{Q}$ (diced) lattice as a function of  $v$  in the region close to  $v = v_c$ . We show the data for (from top to bottom on the left)  $L = 128$  (red),  $L = 256$  (blue),  $L = 384$  (pink), and  $L = 512$  (orange). The black point shows our best estimate for the parameters, as well as their corresponding error bars. The curves shown are our preferred fits with  $(\gamma/v)_{\text{stagg}}$  and  $v$  fixed to the exact values  $26/15$  and  $5/6$ .

For each lattice, we measured the staggered susceptibility  $\chi_{\text{stagg}}$  and the Binder cumulant  $R_{\text{stagg}} = \langle \mathcal{M}_{\text{stagg}}^4 \rangle / \langle \mathcal{M}_{\text{stagg}}^2 \rangle^2$ . The qualitative behavior of these observables is the same for all four lattices considered here. As an example, we show in Fig. 4 the data for the scaled staggered susceptibility of the  $\mathcal{Q}$ (diced) lattice, together with our preferred FSS fits based on the ansatz (3) with a varying number of terms. Since our results for the critical exponents were compatible with the predicted values  $(\gamma/v)_{\text{stagg}} = 26/15$  and  $v = 5/6$  [6], we then refit the fits fixing these parameters to the predicted values, in order to obtain improved estimates for  $v_c$ . Our results are shown in Table III, and agree well with the prediction that the model lies in the universality class of the three-state Potts ferromagnet.

For the lattice  $\mathcal{Q}$ (diced) we have checked directly from the MC simulations that, even though the two sublattices  $G_0$  and  $G_1$  have the same vertex density, it is the diced sublattice  $G_0$  (black vertices in Fig. 2) that becomes ordered. More precisely, the sublattice of  $G_0$  consisting of degree-6 vertices is the one that is most ordered; the two degree-3 sublattices of  $G_0$  are

TABLE III. Critical temperature  $v_c$ , critical exponents  $(\gamma/v)_{\text{stagg}}$  and  $v$ , and critical value of the Binder cumulant  $R_{\text{stagg,c}}$  for the three-state Potts AF on quadrangulations  $\Gamma$  of non-self-dual type. We also include for comparison the results for the diced lattice  $\mathcal{Q}$ (tri) [14]. Estimates of  $v_c$  are the improved estimates based on fixing  $(\gamma/v)_{\text{stagg}} = 26/15$  and  $v = 5/6$ . The last line (“Prediction”) shows the values for the three-state Potts ferromagnet [35,36].

$\Gamma$	$v_c$	$(\gamma/v)_{\text{stagg}}$	$v$	$R_{\text{stagg,c}}$
$\mathcal{Q}$ (diced)	-0.94075(12)	1.737(6)	0.83(7)	1.17(2)
$\mathcal{Q}$ (martini)	-0.77454(6)	1.735(4)	0.83(3)	1.16(1)
$\mathcal{Q}$ (ruby)	-0.95588(9)	1.737(5)	0.80(5)	1.15(3)
$G_3''$	-0.72278(2)	1.736(4)	0.82(2)	1.17(1)
Diced	-0.860599(4)	1.737(4)	0.81(2)	1.170(7)
Prediction		26/15	5/6	1.1711(5)

TABLE IV. Real roots of  $P_B(3, v)$ , to 20-digit numerical precision, for  $\mathcal{Q}$ (diced). We show the unique real root  $v_c(n)$  in the AF interval  $v \in [-1, 0)$ , for  $n \times \infty$  bases, together with the extrapolation to  $n = \infty$  (where we used exponents in the range 1.2–1.5, which are much smaller than those for the ferromagnetic models investigated in Refs. [27,37,38]).

$n$	$v_c(n)$
2	-0.93449469491145567949
4	-0.93889690618313817225
6	-0.93976678350525022210
8	-0.94017098791714722205
10	-0.94038789257375557598
12	-0.94051494788357303489
$\infty$	-0.94080(1)

slightly more ordered than the three sublattices of the kagome sublattice  $G_1$ . Therefore, although both sublattices  $G_0$  and  $G_1$  give naively the same entropy density, it is the one having a sub-sublattice with the largest degree that becomes ordered, because fluctuations around these three ideal states maximize the system’s entropy density. A similar phenomenon occurs for the  $\mathcal{Q}$ (ruby) lattice [28].

On all these lattices (as well as on the diced lattice [14]), the WSK algorithm suffers from CSD, with dynamic critical exponents  $z_{\text{int}, \mathcal{M}_{\text{stagg}}^2} = 0.50(1)$  and  $z_{\text{int}, \mathcal{M}_q^2} = 0.48(1)$ . If these exponents are in fact equal, then our preferred estimate (taking into account the statistical nonindependence of the two estimates) would be  $z_{\text{int}} = 0.49(2)$ . This is compatible with the exponent  $z_{\text{int}, \mathcal{M}^2} = 0.475(6)$  found in the Swendsen-Wang (SW) algorithm [34] for the three-state Potts ferromagnet [35,36].

Finally, we have applied the CP method [27,37,38] to study the location of the critical point for the three-state Potts AF on the  $\mathcal{Q}$ (diced) lattice. We computed the CP  $P_B(3, v)$  for some bases  $B$  that admit a four-terminal representation (to be able to use the TM method of Ref. [37]). In particular, to compute the estimates of  $v_c$  shown in Table IV, we have used the more powerful eigenvalue method of Ref. [38], which allows us to use bases of size  $n \times m$  in the limit  $m \rightarrow \infty$ . The last row of Table IV shows the extrapolation to  $n = \infty$  using Monroe’s implementation of the Bulirsch-Stoer [39] extrapolation scheme. This result agrees within errors with the MC estimate, but it is more precise.

#### IV. CONCLUSIONS

We have studied the three-state Potts AF on four quadrangulations of self-dual type, and on four quadrangulations of non-self-dual type (including two with equal vertex densities on the two sublattices), by extensive computations using MC simulations, TM computations, and the CP method. In all cases, we have found a perfect agreement with Conjecture 1. Our findings provide very strong empirical support for the validity of this criterion. However, we do not want to exclude the possibility that for some lattices of non-self-dual type the finite-temperature transition might be first order.

As a side result, we have also found that the WSK algorithm has no CSD when simulating the three-state Potts AF on any quadrangulation of self-dual type, while it has CSD

(compatible with the dynamic universality class of the SW algorithm for the three-state ferromagnet) on any quadrangulation of non-self-dual type.

### ACKNOWLEDGMENTS

We thank Kun Chen and Yuan Huang for their participation in an early stage of this work. This work was supported in part by the Natural Science Foundation of China Grants

No. 11625522, No. 11405003, and No. 11774002, the Key Projects of Anhui Province University Outstanding Youth Talent Support Program Grant No. gxyqZD2017009, the Ministry of Science and Technology of China Grant No. 2016YFA0301600, the Institut Universitaire de France, the European Research Council through the Advanced Grant NuQFT, the Spanish MINECO FIS2014-57387-C3-3-P and MINECO/AEI/FEDER, UE FIS2017-84440-C2-2-P grants, and EPSRC Grant No. EP/N025636/1.

- 
- [1] H. A. Kramers and G. H. Wannier, *Phys. Rev.* **60**, 252 (1941).  
 [2] R. Savit, *Rev. Mod. Phys.* **52**, 453 (1980).  
 [3] J. Polchinski, *Rev. Mod. Phys.* **68**, 1245 (1996).  
 [4] R. B. Potts, *Proc. Cambridge Philos. Soc.* **48**, 106 (1952).  
 [5] F. Y. Wu, *Rev. Mod. Phys.* **54**, 235 (1982); **55**, 315(E) (1983); *J. Appl. Phys.* **55**, 2421 (1984).  
 [6] R. J. Baxter, *Exactly Solved Models in Statistical Mechanics* (Academic, New York, 1982).  
 [7] B. Nienhuis, *J. Stat. Phys.* **34**, 731 (1984).  
 [8] P. Di Francesco, P. Mathieu, and D. Sénéchal, *Conformal Field Theory* (Springer, New York, 1997).  
 [9] C. L. Henley (unpublished).  
 [10] J. Kondev and C. L. Henley, *Nucl. Phys. B* **464**, 540 (1996).  
 [11] J. K. Burton, Jr. and C. L. Henley, *J. Phys. A* **30**, 8385 (1997).  
 [12] J. Salas and A. D. Sokal, *J. Stat. Phys.* **92**, 729 (1998), and references therein.  
 [13] J. L. Jacobsen, in *Polygons, Polyominoes and Polycubes*, edited by A. J. Guttmann, Lecture Notes in Physics Vol. 775 (Springer, Dordrecht, 2009), Chap. 14.  
 [14] R. Kotecký, J. Salas, and A. D. Sokal, *Phys. Rev. Lett.* **101**, 030601 (2008).  
 [15] M. P. M. den Nijs, M. P. Nightingale, and M. Schick, *Phys. Rev. B* **26**, 2490 (1982).  
 [16] J. Kolafa, *J. Phys. A* **17**, L777 (1984).  
 [17] R. Kotecký, A. D. Sokal, and J. M. Swart, *Commun. Math. Phys.* **330**, 1339 (2014).  
 [18] J. L. Jacobsen and J. Salas (unpublished).  
 [19] Y. Huang, K. Chen, Y. Deng, J. L. Jacobsen, R. Kotecký, J. Salas, A. D. Sokal, and J. M. Swart, *Phys. Rev. E* **87**, 012136 (2013).  
 [20] J. Ashley, B. Grünbaum, G. C. Shephard, and W. Stromquist, in *Applied Geometry and Discrete Mathematics* (American Mathematical Society, Providence, RI, 1991), pp. 11–50.  
 [21] M. O’Keeffe, *Aust. J. Chem.* **45**, 1489 (1992).  
 [22] M. O’Keeffe and B. G. Hyde, *Crystal Structures I. Patterns and Symmetry* (Mineralogical Society of America, Washington, DC, 1996), Sec. 5.3.7.  
 [23] B. Servatius and H. Servatius, in *Proceedings of the International Scientific Conference on Mathematics* (Žilina, 30 June–3 July 1998), edited by V. Bálint (University of Žilina, Žilina, 1998), pp. 83–116.  
 [24] J. C. Wierman, in Proceedings of the 5th Hawaii International Conference on Statistics, Mathematics and Related Fields, 2006 (unpublished).  
 [25] C. R. Scullard, *Phys. Rev. E* **73**, 016107 (2006).  
 [26] R. M. Ziff, C. R. Scullard, J. C. Wierman, and M. R. A. Sedlock, *J. Phys. A* **45**, 494005 (2012).  
 [27] J. L. Jacobsen and C. R. Scullard, *J. Phys. A* **45**, 494003 (2012); C. R. Scullard and J. L. Jacobsen, *ibid.* **45**, 494004 (2012); J. L. Jacobsen and C. R. Scullard, *ibid.* **46**, 075001 (2013); C. R. Scullard and J. L. Jacobsen, *ibid.* **49**, 125003 (2016).  
 [28] J. P. Lv, Y. Deng, J. L. Jacobsen, and J. Salas (unpublished).  
 [29] J.-S. Wang, R. H. Swendsen, and R. Kotecký, *Phys. Rev. Lett.* **63**, 109 (1989); *Phys. Rev. B* **42**, 2465 (1990).  
 [30] S. J. Ferreira and A. D. Sokal, *J. Stat. Phys.* **96**, 461 (1999).  
 [31] B. Mohar, in *Graph Theory in Paris*, edited by J. A. Bondy *et al.* (Birkhäuser, Basel, 2007), pp. 287–297.  
 [32] H. W. J. Blöte, J. L. Cardy, and M. P. Nightingale, *Phys. Rev. Lett.* **56**, 742 (1986).  
 [33] I. Affleck, *Phys. Rev. Lett.* **56**, 746 (1986).  
 [34] R. H. Swendsen and J.-S. Wang, *Phys. Rev. Lett.* **58**, 86 (1987).  
 [35] J. Salas and A. D. Sokal, *J. Stat. Phys.* **87**, 1 (1997).  
 [36] T. M. Garoni, G. Ossola, M. Polin, and A. D. Sokal, *J. Stat. Phys.* **144**, 459 (2011).  
 [37] J. L. Jacobsen, *J. Phys. A* **47**, 135001 (2014).  
 [38] J. L. Jacobsen, *J. Phys. A* **48**, 454003 (2015).  
 [39] R. Burlisch and J. Stoer, *Numer. Math.* **6**, 413 (1964); J. L. Monroe, *Phys. Rev. E* **65**, 066116 (2002).